Clinical assessment of the development of hypertrophic cardiomyopathy by cardiovascular magnetic resonance imaging

Brouwer, W.P.

2014

document version
Publisher's PDF, also known as Version of record

V

Crypts predict the hypertrophic response in HCM mutation carriers.

Wessel P. Brouwer, Tjeerd Germans, Maaike C. Head, Otto Kamp, Mohamed F.A. Aly, Arthur A.M. Wilde, Jolanda van der Velden, Albert C. van Rossum

Submitted

Abstract

Objectives

We used serial cardiovascular magnetic resonance imaging (CMR) in mutation carriers to monitor LV mass, LV function, LV morphology and left atrial (LA) volumes to gain insight in the natural course of development of HCM.

Background

Hypertrophic cardiomyopathy (HCM) is characterized by the development of left ventricular (LV) hypertrophy in the absence of increased loading conditions. Genetic testing has identified an increasing number of HCM mutation carriers, in whom no or only mild hypertrophy is present (mutation carriers). Insight in the development of LV remodeling is mandatory to develop effective treatment strategies to prevent HCM. However, clinical, non-invasive markers to predict LV hypertrophy are scarce.

Methods

Serial CMR acquisitions with cine SSFP imaging were performed in 27 mutation carriers (11 male, age 4±3 years) of mutations in the *MYBPC3* (n=22) and *TPM1* (n=5) gene.

Results and conclusions

After a mean follow-up duration of 4.8±0.9 years, LV mass (corrected for body surface area) increased significantly from 45±9 $g \cdot m^{-2}$ to 48±8 $g \cdot m^{-2}$ (p=0.001). Also, maximal and minimal LA dimensions showed a significant increase (54±11 $mL \cdot m^{-2}$ vs 58±10 $mL \cdot m^{-2}$, $p<0.01$ and 24±6$mL \cdot m^{-2}$ vs 29±7 $mL \cdot m^{-2}$, $p<0.001$, respectively). Regression analysis revealed the presence of intramyocardial crypts to be an independent predictor for the increase of LV mass (r=0.51, p=0.01). During 5 year follow-up, crypts were an independent predictor of increase in LV mass in mutation carriers with no or mild LV hypertrophy. Therefore, the presence of crypts may identify mutation carriers who are more prone to develop overt HCM and may warrant more intensive monitoring.

Introduction

Hypertrophic cardiomyopathy (HCM) is caused by mutations in genes that encode for structural and regulatory proteins of the sarcomere and is mainly characterized by asymmetric left ventricular (LV) hypertrophy. HCM is associated with adverse clinical outcome, such as heart failure, embolic stroke due to atrial fibrillation, development of ventricular arrhythmias and subsequent sudden cardiac death (SCD) [1-3]. Since HCM has a Mendelian trait of inheritance [4], genetic testing has become an important tool to identify affected individuals (mutation carriers) among asymptomatic family members of index HCM patients. As HCM is relatively common (the prevalence is estimated to be 1:500 in the general population [1]) and genetic screening tools have become cost efficient [5] and readily available, an increasing number of mutation carriers without LV hypertrophy are identified. Intensive monitoring of all mutation carriers would be a heavy burden on healthcare budgets with potentially limited clinical benefit[6]. In addition, thus far, trials on reducing hypertrophy in overt HCM patients have failed to show favourable results. Therefore, the focus of research has shifted from reduction of LV hypertrophy in overt HCM to the development of preventive treatment strategies in mutation carriers with limited LV hypertrophy. Since HCM only develops in two thirds of mutation carriers [4], it is very important to identify those mutation carriers who are likely to benefit most from, presumably, life long therapy.

Mutation carriers with limited hypertrophy have shown to display morphological and functional abnormalities, such as left atrial (LA) dilation, subtle signs of diastolic dysfunction [7,8], intramyocardial crypts, and late gadolinium enhancement using cardiovascular magnetic resonance imaging (CMR) [9,10]. CMR has also been shown to be superior to 2D echocardiography in diagnosing localized hypertrophy in HCM

[11]. The aim of this study was to use CMR in mutation carriers to monitoring LV and LA remodelling, and to identify predictors for the development of LV hypertrophy.

Methods

Patients

Mutation carriers comprised of individuals harbouring a founder mutation (2373insG) in the gene encoding myosin binding protein C3 *(MYBPC3)* or α*(TPM1)*, as previously described[7]. Subjects underwent baseline and follow-up CMR examinations. Directly after CMR, a twelve-lead electrocardiogram was performed in each mutation carrier. Mutation carriers were selected for the study when baseline echocardiography (which was performed within a year before baseline CMR acquisition) revealed a maximal LV wall thickness not exceeding 10 mm, indicating that mutation carriers were in a pre-hypertrophic state at baseline. A subset of mutation carriers also underwent echocardiographic examinations, just prior or directly after the CMR acquisition, in order to minimize differences in hemodynamics between both acquisitions. Study participants had to be in sinus rhythm with minimum age of 18 years. All mutation carriers gave written informed consent. The study was conducted according to the declaration of Helsinki after the approval by the institutional medical ethics committee.

Controls

Controls consisted of gender-matched family members in whom no sarcomeric gene mutations were found by genetic analysis. All controls satisfied the following criteria: normal echocardiogram, normal electrocardiogram, no cardiac history of cardiac

symptoms, no hypertension or diabetes, no use of cardiac medication and no abnormalities during physical examination.

CMR image acquisition

Both baseline and follow-up CMR examinations were performed on a single 1.5 T whole body scanner (Magnetom Sonata, Siemens, Erlangen, Germany) with a 32 channel phased array body coil. A standard protocol with long- and short-axis cine imaging were performed with a retrospective gated steady state free precession (SSFP) sequence after the acquisition of standard localizing scans. Subsequently, a modified two-chamber cine image was planned through the inferoseptum, which has been shown to be the optimal image plane for the visualisation of inferoseptal crypts [9]. Intramyocardial crypts were defined as abrupt invaginations of normally contracting myocardium, penetrating the LV wall for a minimum of 30%, as described previously [10].

A transverse stack of cine images was planned with full coverage of the LA, in order to derive maximal and minimal LA volumes during the cardiac cycle, as described previously [12]. Late gadolinium enhancement (LGE) images were obtained approximately ten minutes after the intravenous administration of a weight-dependant (0.2 mmol/kg) bolus of Gadolinium-DTPA (Magnevist ©, Schering). LGE images were obtained in the end-diastolic phase and planned at identical image positions as the long- and short axis SSFP cine images. For each separate acquisition, image quality was optimized by applying an inversion recovery time typically within a range of 250-320ms.

Off-line CMR analysis

Dedicated software (Mass, Medis, Leiden, the Netherlands) was used to quantify LV volumes and mass and to determine LA volumes. LV volumes were determined after delineation of the endocardial borders of short-axis images in end-diastolic (ED) and end-systolic (ES) phase. LV mass was assessed by drawing both epi- and endocardial ED contours, including the papillary muscles. From these measurements, LV end diastolic volume (LVEDV), LV end systolic volume (LVESV), stroke volume (SV), LV ejection fraction (LVEF), and LV mass to LVEDV ratio were obtained. LA volumes were assessed as described previously [12]. All volumetric parameters were indexed to body surface area (BSA). Maximal LV wall thickness (WT) was determined on ED short-axis cine images. All maximal LVWT measurements were performed on identical regions of the LV at baseline and follow-up. The presence of crypts was assessed by careful evaluation of both long-axis and modified two-chamber cine images, and subsequently scored according to their number and the relative penetration into the myocardium, as described previously [10]. LGE images were visually evaluated for the presence of fibrosis by two independent experienced CMR reviewers (T.G. and W.B).

Electrocardiography

Standard twelve-lead electrocardiograms were evaluated for the presence of LV hypertrophy (by the Romhilt-Estes criteria [13], abnormal r-amplitudes in lead V1 (>3mm), q-waves in the anterolateral leads with >3mm depth and/or >0.04s in duration [14], deviating ST-segments [15] and conduction abnormalities.

Echocardiography

Echocardiographic examinations were performed in a subset of mutation carriers using either a General Electrics Vivid-7 (GE Vingmed Ultrasound, Horten, Norway) ultrasound device or a Philips iE33 (Philips Medical Systems, Best, The Netherlands). Tissue Doppler imaging (TDI) was applied on apical 4-chamber views and sample volumes of myocardial tissue at the septal and lateral borders of the mitral valve were selected. Special care was taken to align the direction of motion with the ultrasound beam (<15 degrees angle was considered agreeable for analysis). A frame rate of 75/s minimum was used to determine the peak systolic (Sa), peak early diastolic (Ea) and peak late diastolic (Aa) velocities at both junctions.

Statistical analysis

Statistical analysis was performed using a SPSS 15.0 for Windows (SPSS Inc, Chicago, IL). All continuous variables are presented as mean±SD. Data between baseline and follow-up were compared using a paired Student's t-test. In case of abnormal distribution, non-parametric testing was used for comparison. Between groups, variables were compared with an independent Student's t-test. Linear regression analysis was applied to correlate changes in CMR variables (i.e. LV mass, maximal LVWT, LV mass-to–LV end-diastolic volume (EDV) ratio, maximal and minimal LA volumes) to gender, age, type of mutation, baseline LVEDV, baseline LVESV, baseline minimal and maximal LA volumes and the presence or absence of crypts. Moreover, correlations of the previously mentioned CMR variables to baseline TDI velocities were made in a subset of mutation carriers with *MYBPC3*-mutations only. Two-sided p-values < 0.05 were considered statistically significant.

Results

Mutation carriers and controls

In total, 28 mutation carriers were included of whom 23 had a *MYBPC3* founder mutation (2373insG) and 5 had a α-tropomyosin mutation (Glu62Gln). One female mutation carrier with a *MYBPC3* gene mutation declined further participation. In one *MYBPC3* mutation carrier, the stack of LA cine images was incomplete at follow-up. Therefore, complete LV and LA datasets of 27 and 26 mutation carriers were included in the analysis, respectively. The mean duration of follow-up was 4.8±0.9 years. Baseline demographic and clinical data from mutation carriers and family members (n=11, 6 male, mean age 50±8 years) are described in Table 1. As shown, controls were significantly older than mutation carriers, but equally matched for gender. The mean duration of follow-up was 4.8±0.9 years.

Table 1. Baseline characteristics of mutation carriers and controls.

Variable	Mutation carriers (n=27)	Controls (n=11)
Age (years)	40±13	50±8*
Gender (male / female)	11 / 16	6 / 5
Sarcomeric gene mutation:		
MYBPC3 (n, %)	22 (81)	None
TPM1 (n, %)	5 (19)	
Systolic blood pressure (mmHg)	118±12	124±10
Diastolic blood pressure (mmHg)	69±9	77±5†
Heart rate (bpm)	64±10	68±9

MYBPC3= myosin binding protein C. *TPM1*=α-tropomyosin. * $p<0.05$, † $p<0.01$.

LV remodelling

As shown in Table 2, LV mass was comparable between mutation carriers and controls at baseline, but LV mass increased significantly in mutation carriers during follow-up from 45±9 g·m^{-2} to 48±8 g·m^{-2} (p=0.001). Also, both maximum LV wall thickness and LV mass-to–LVEDV ratio changed significantly over time (from 12±3 mm to 13±4 mm, p=0.01 and from 0.5±0.08 to 0.6±0.09, p<0.001, respectively). LV volumes and ejection fraction remained unchanged.

Table 2. Serial CMR findings in mutation carriers and controls.

Variable	Mutation carriers		Controls	
	Baseline	Follow-up	Baseline	Follow-up
LVEDV (mL·m^{-2})	89±11	86±8	91±18	85±14§
LVESV (mL·m^{-2})	37±6	36±6	35±10	36±9
LVEF (%)	59±4	58±5	61±7	59±5
LV mass (g·m^{-2})	45±9	48±8†	45±7	43±4
LVWT (mm)	12±3‡	13±4*||¶	10±1	10±1
LV mass-to–LVEDV ratio	0.5±0.08	0.6±0.09‡	0.5±0.06	0.5±0.08
Crypts (n,%)	16/24, 67	20/27, 74	None	None
Median number of crypts	3±2	3±2		
Crypt penetrance (%)	75±24	71±23		
Maximum LA volume (mL·m^{-2})	54±11	58±10†¶	49±8	50±9
Minimum LA volume (mL·m^{-2})	24±6	29±7‡#	22±4	22±4

EDV=end-diastolic volume. ESV=end-systolic volume. EF=ejection fraction. WT=wall thickness. * p<0.05 vs carriers at baseline, † p<0.01 vs carriers at baseline, ‡ p<0.001 vs carriers at baseline, § p<0.05 vs controls at baseline, || p<0.01 vs controls at baseline, ¶ p<0.05 vs controls at follow-up, # p<0.01 vs controls at follow-up.

Crypt formation

At baseline, modified two-chamber views were not performed in 3 mutation carriers, resulting in 24 patients which were eligible for comparison of crypt characteristics. Of these patients, 16 (67%) were crypt positive. At follow-up, complete imaging protocols for the detection of crypts were available in 27 patients, revealing crypts in 20 (74%) of patients. The prevalence of crypts and the crypt characteristics (median number and penetrance) remained constant, as shown in Table 2. No crypts were present in controls.

Late gadolinium enhancement

In three mutation carriers, patchy LGE was present at baseline, indicating intramyocardial fibrosis. None of the LGE positive mutation carriers showed enlargement of the myocardial areas with LGE over time. No LGE negative carriers developed myocardial areas with LGE during follow-up.

LA volumes

Maximal and minimal LA dimensions increased significantly between baseline and follow-up (from 54±11 $mL \cdot m^{-2}$ to 58±10 $mL \cdot m^{-2}$, $p<0.01$ and from 24±6 $mL \cdot m^{-2}$ to 29±7 $mL \cdot m^{-2}$, $p<0.001$, respectively). In genotype negative family members, LA dimensions remained constant over time (see Table 2).

Predictors of LV and LA remodelling in carriers

After univariate regression analysis, the only significant predictor for the increase in LVmass over time was the presence of crypts (r.=0.51, p=0.01). Gender, age, type of sarcomeric mutation, baseline LV volumes and baseline minimal and maximal LA

volumes all failed to show significant relationships. The differences in evolution of LV mass between crypt positive and crypt negative mutation carriers are outlined in Figure 1. No significant predictors were found for changes in maximal LVWT and LV mass-to–LVEDV ratio. Changes in maximal LA volume were predicted by baseline LVEDV values (r.=0.52, p<0.01). No predictors were found for changes in minimal LA volume.

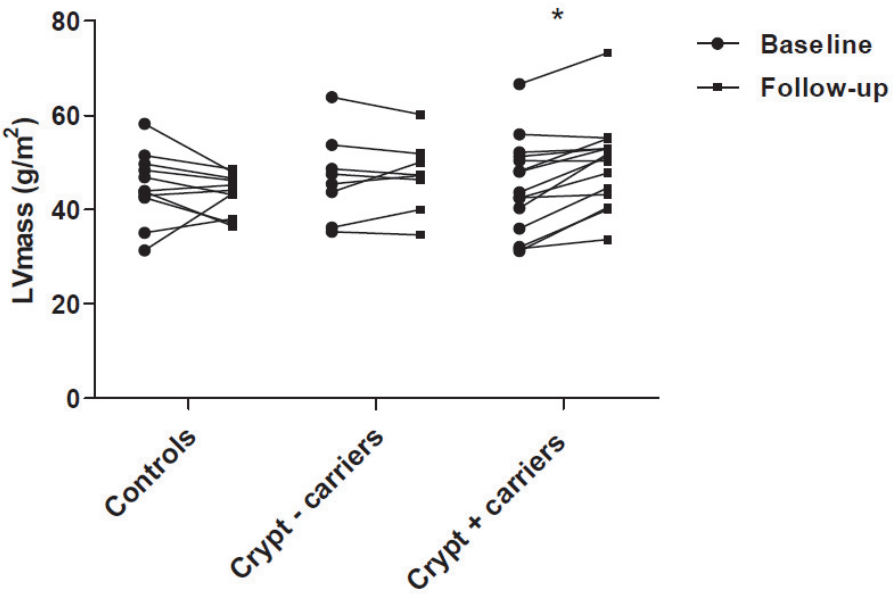

Figure 1. Differences in evolution of LV mass (corrected for body surface area) between controls, crypt-positive and crypt-negative mutation carriers. Solely within the group of crypt-positive mutation carriers, the increase of (indexed) LV mass was significant over time. * p=0.01.

Echocardiography

In twelve mutation carriers with *MYBPC3* gene mutations, echocardiographic TDI examinations were performed at both time points, as shown in Table 3. Septal Ea decreased significantly over time; from 10.3±2.6 cm·s^{-1} towards 8.7±2.6 cm·s^{-1}, p<0.001, while lateral Sa showed an increase; from 8.9±1.7 towards 10.4±2.8, p<0.05. Baseline lateral Aa showed a positive correlation with changes in LV mass (r.=0.69, p=0.01).

Table 3. Differences in TDI parameters over time in mutation carriers.

TDI velocities	Baseline (n=12)	Follow-up (n=12)
Septal Sa (cm·s^{-1})	9.1±1.9	8.6±2.0
Ea (cm·s^{-1})	10.3±2.6	8.7±2.6†
Aa (cm·s^{-1})	8.2±1.6	8.2±1.3
Lateral Sa (cm·s^{-1})	8.9±1.7	10.4±2.8*
Ea (cm·s^{-1})	13.6±3.9	12.7±3.6
Aa (cm·s^{-1})	9.0±2.2	10.1±2.6

* p<0.05, † p<0.001.

Electrocardiography

None of the mutation carriers showed electrocardiographic evidence of left ventricular hypertrophy (LVH) according to the Romhilt-Estes criteria [13] at baseline or during follow-up. Abnormal r-waves in V1 were present in 6 mutation carriers and showed no changes over time. Noteworthy, 5 (83%) of these individuals carried a α-tropomyosin mutation. Two mutation carriers (one *MYBPC3*, one *TPM1*) showed abnormal q-waves at baseline. Interestingly, one of these carriers showed LGE at the inferoseptum. During follow-up, abnormal q-waves appeared in one

additional *MYBPC3* carrier, who showed no LGE. Deviating ST-segments were present in 3 mutation carriers at baseline, and in 1 additional mutation carrier during follow-up. Conduction abnormalities consisted of incomplete right bundle branch block (iRBBB, n=2) and first-degree atrioventricular conduction delay at baseline (n=1). At follow-up, 4 patients showed an iRBBB and no first-degree conduction delays were seen. Off note, ECG abnormalities at baseline failed to predict LV and LA remodelling (data not shown).

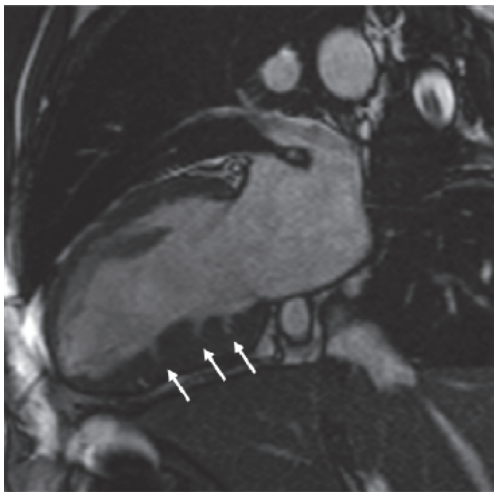

Figure 2. Intramyocardial crypts in an asymptomatic mutation carrier. This modified two-chamber cine image shows deep penetrating crypts at the basal and mid-ventricular inferoseptum (white arrows) in a carrier of an α-tropomyosin (TPM1) mutation.

Discussion

The present CMR study demonstrated that in middle aged mutation carriers, both LV and LA remodelling occur after a follow-up duration of approximately 5 years. Importantly, the presence of intramyocardial crypts was an independent predictor for the increase in LV mass. It must be noted however, that no predictors were found for the regional hypertrophic response in these patients. None of the mutation

carriers showed new myocardial areas with LGE during follow-up. The increase in LA volumes corresponded with a decrease in early diastolic myocardial TDI velocities.

Nowadays, CMR may be regarded as first-choice imaging modality to monitor HCM, since CMR allows to identify regional hypertrophy that remains undetected with standard echocardiography [11] and allows visualization of macroscopic areas of interstitial fibrosis with LGE. From previous longitudinal studies, it is known that in mutation carrriers who harbour a mutation in the *MYBPC3* gene, penetration of HCM occurs predominantly from the third or fourth decade of life [16-18]. This is in line with our study findings; over a third of our mutation carrier population, of which the majority carried a *MYBPC3* gene mutation and had mean age of 40±13 years, had localized LV hypertrophy on CMR (data not shown). Additionally, 4% of patients developed manifest HCM during follow-up. These newly diagnosed HCM patients all had normal LV wall thickness on echocardiography, indicating the incremental value to use CMR for monitoring HCM.

We found that a reduction of early diastolic TDI myocardial velocities was inversely related to an increase in LV mass, which is in line with previous reports [19]. Late diastolic velocities of the lateral mitral annulus (e.g. lateral Aa) on the other hand positively correlated with an increase in LV mass. Michels et al. [20] previously demonstrated that a large proportion of mutation carriers with comparable age profile shows isolated increased Aa velocities at various sites of the mitral annulus. Abnormal late diastolic movement of the mitral annulus therefore not only seems to serve as an early sign of abnormal relaxation in HCM, and may be a marker of disease development [21]. Also, we found an increase in LA volumes related to an increase of LV mass, which is in line with previous reports.

Interestingly, we found that the presence of intramyocardial crypts at baseline was an independent predictor for the progression of LV mass in our study population of mutation carriers. We hypothesize that crypts, which are the presumed overt manifestation of extensive localized disarray at the inferoseptal area [21], may induce compensatory hypertrophy due to alterations in regional contractility and disrupted effective myocardial architecture. Indeed, we have recently demonstrated that the Frank-Starling mechanism is impaired in mutation carriers [7,22]. However, future studies are needed however to unravel the exact mechanism of this association. The observation that crypts failed to regress in frequency and number despite an ongoing process of LV wall thickening corresponds to the high prevalence of crypts we observed in a group of manifest HCM patients (unpublished data).

Electrocardiographic abnormalities, which are described to precede hypertrophic development in HCM [23], also remained constant over time, indicating that follow-up with electrocardiography alone is too insensitive to detect HCM disease progression.

Study limitations and clinical implications

The study population was rather small and mainly consisted of carriers of *MYBPC* founder mutations. Therefore, prudence to extrapolate these results to a general HCM population is warranted and future multicenter studies with large demographic variation are needed, to definitely establish the prognostic importance of crypts in HCM. Another study limitation was that crypts solely predicted an increase in global LV mass and not regional LV hypertrophy, with LV mass still within the normal range at follow-up. As a result, the transition of pre-hypertrophic mutation carriership towards manifest HCM was difficult to assess in our study, further hampered by the

observation that an important amount of mutation carriers already had localized LV hypertrophy at baseline, which was missed by echocardiography. Finally, TDI was solely performed in a subset of carriers with *MYBPC3* gene mutations. Therefore, TDI data are applicable to these specific mutation carriers only.

In conclusion, CMR is an important and accurate tool to monitor LV wall thickness, LV mass and left atrial remodelling in HCM mutation carriers. Our CMR-study with ~5 year follow-up showed that the presence of crypts was an independent predictor for increase of LV mass in these patients. Therefore, crypts may be used to identify patients at risk for an accelerated hypertrophic response, which may warrant closer monitoring of this particular subset of mutation carriers. Larger studies with extensive follow-up are nevertheless needed to address this issue.

References

1. Maron BJ. Hypertrophic Cardiomyopathy: A Systematic Review. *JAMA* 2002;287:1308-1320.

2. Maron BJ, Olivotto I, Bellone P et al. Clinical profile of stroke in 900 patients with hypertrophic cardiomyopathy. *J Am Coll Cardiol* 2002;39:301-307.

3. Maron BJ. Sudden death in hypertrophic cardiomyopathy. *J Cardiovasc Transl Res* 2009;2:368-380.

4. Marian AJ, Roberts R. Molecular genetic basis of hypertrophic cardiomyopathy: genetic markers for sudden cardiac death. *J Cardiovasc Electrophysiol* 1998;9:88-99.

5. Ingles J, McGaughran J, Scuffham PA, Atherton J, Semsarian C. A cost-effectiveness model of genetic testing for the evaluation of families with hypertrophic cardiomyopathy. *Heart* 2012;98:625-630.

6. Christiaans I, Dijksman LM, Birnie E. ESCAPE-HCM study: Evaluation of SCreening of Asymptomatic PatiEnts with Hypertrophic CardioMyopathy. *Neth Heart J* 2007;15:216-220.

7. Germans T, Russel IK, Gotte MJ et al. How do hypertrophic cardiomyopathy mutations affect myocardial function in carriers with normal wall thickness? Assessment with cardiovascular magnetic resonance. *J Cardiovasc Magn Reson* 2010;12:13.

8. Nagueh SF, Bachinski LL, Meyer D et al. Tissue Doppler imaging consistently detects myocardial abnormalities in patients with hypertrophic cardiomyopathy and provides a novel means for an early diagnosis before and independently of hypertrophy. *Circulation* 2001;104:128-130.

9. Germans T, Wilde AAM, Dijkmans PA et al. Structural Abnormalities of the Inferoseptal Left Ventricular Wall Detected by Cardiac Magnetic Resonance Imaging in Carriers of Hypertrophic Cardiomyopathy Mutations. *J Am Coll Cardiol* 2006;48:2518-2523.

10. Brouwer WP, Germans T, Head MC et al. Multiple myocardial crypts on modified long-axis view are a specific finding in pre-hypertrophic HCM mutation carriers. *Eur Heart J Cardiovasc Imaging* 2012;292-297.

11. Rickers C, Wilke NM, Jerosch-Herold M et al. Utility of Cardiac Magnetic Resonance Imaging in the Diagnosis of Hypertrophic Cardiomyopathy. *Circulation* 2005;112:855-861.

12. Germans T, Götte MJW, Nijveldt R et al. Effects of Aging on Left Atrioventricular Coupling and Left Ventricular Filling Assessed Using Cardiac Magnetic Resonance Imaging in Healthy Subjects. *Am J Cardiol* 2007;100:122-27.

13. Romhilt DW, Bove KE, Norris RJ et al. A Critical Appraisal of the Electrocardiographic Criteria for the Diagnosis of Left Ventricular Hypertrophy. *Circulation* 1969;40:185-196.

14. Konno T, Shimizu M, Ino H et al. Diagnostic value of abnormal Q waves for identification of preclinical carriers of hypertrophic cardiomyopathy based on a molecular genetic diagnosis. *Eur Heart J* 2004;25:246-251.

15. Lakdawala NK, Thune JJ, Maron BJ et al. Electrocardiographic Features of Sarcomere Mutation Carriers With and Without Clinically Overt Hypertrophic Cardiomyopathy. *Am J Cardiol* 2011;108:1606-1613.

16. Spirito P, Maron BJ. Absence of progression of left ventricular hypertrophy in adult patients with hypertrophic cardiomyopathy. *J Am Coll Cardiol* 1987;9:1013-1017.

17. Maron BJ, Niimura H, Casey SA et al. Development of left ventricular hypertrophy in adults with hypertrophic cardiomyopathy caused by cardiac myosin-binding protein C gene mutations. *J Am Coll Cardiol* 2001;38:315-321.

18. Niimura H, Bachinski LL, Sangwatanaroj S et al. Mutations in the Gene for Cardiac Myosin-Binding Protein C and Late-Onset Familial Hypertrophic Cardiomyopathy. *N Engl J Med* 1998;338:1248-1257.

19. Nagueh SF, McFalls J, Meyer D et al. Tissue Doppler imaging predicts the development of hypertrophic cardiomyopathy in subjects with subclinical disease. *Circulation* 2003;108:395-398.

20. Michels M, Soliman OII, Kofflard MJ et al. Diastolic Abnormalities as the First Feature of Hypertrophic Cardiomyopathy in Dutch Myosin-Binding Protein C Founder Mutations. *JACC: Cardiovasc Imag* 2009;2:58-64.

21. Kuribayashi T, Roberts WC. Myocardial disarray at junction of ventricular septum and left and right ventricular free walls in hypertrophic cardiomyopathy. *Am J Cardiol* 1992;70:1333-1340.

22. Sequeira V, Wijnker PJ, Nijenkamp LL et al. Perturbed length-dependent activation in human hypertrophic cardiomyopathy with missense sarcomeric gene mutations. *Circ Res* 2013;112:1491-1505

23. Konno T, Shimizu M, Ino H et al. Differences in Diagnostic Value of Four Electrocardiographic Voltage Criteria for Hypertrophic Cardiomyopathy in a Genotyped Population. *Am J Cardiol* 2005;96:1308-13.